

Electrochemical Oxidation of Dyes on Oxide Lead Anode with the Involvement of Active Oxygen Species

G. V. Kornienko^a, T. A. Kenova^{a*}, V. L. Kornienko^a, O. A. Golubtsova^{a,b}, and N. G. Maksimova^a

^aInstitute of Chemistry and Chemical Technology, Krasnoyarsk Scientific Center, Siberian Branch,
Russian Academy of Sciences, Akademgorodok 50, str. 24, Krasnoyarsk, 660036 Russia

*e-mail: kta@icct.ru

^bSiberian State Aerospace University named after M.F. Reshetnev, ul. Yunost 18, Krasnoyarsk, 660123 Russia

Received September 19, 2017

Abstract—Kinetics and selectivity of oxidation of dyes (Methyl Orange and Chrome Dark Blue) on a lead dioxide (Pb/PbO_2) anode at various current densities, substrate concentrations, and pH values with the use of various active oxygen species was studied. It was shown that the electrochemical oxidation of dyes on the Pb/PbO_2 anode occurs rather effectively under the chosen conditions. The mineralization efficiency in 5 h was 51 to 89.5 and 93 to 100% for, respectively, Methyl Orange and Chrome Dark Blue, depending on the electrolysis conditions.

DOI: 10.1134/S1070427217080079

The problems of ecological safety, associated with the increasing contamination of the air and water basins are currently pressing in many countries all over the world. The conventional approaches in the field of water treatment are frequently poorly efficient in purification and utilization of industrial and household discharges containing toxic, nonbiodegradable, and difficultly oxidizable organic compounds. In this context, water purification technologies based on deep conversion of organic molecules under the action of strong oxidizing agents are promising. To these methods belong chemical and electrochemical processes to give highly reactive intermediates (HO^\bullet , HO_2^\bullet , O_2^\bullet , ClO^\bullet), i.e., the so-called advanced oxidation processes (AOPs) [1–5].

When finding way into water objects even in small amounts, synthetic dyes used in a number of industries, mostly in textile industry, not only raise the water color index, but also make slower the photosynthesis processes and exhibit a toxic effect on the water microflora [6].

Dye-containing wastewater is conventionally purified with the use of various physical, chemical, and biological processes. However, these processes are frequently ecologically or economically inefficient. Oxidative destruction processes, such as ozonization, photo-

oxidation, chemical oxidation by the Fenton reagent, and electrochemical oxidation, have been suggested recently for removing dyes [7–9].

Among AOPs, the electrochemical technologies are the most attractive because of using a “pure reagent,” electron. Electrochemical reactions occur under mild conditions at comparatively high rates, are controlled by the current density and potential, do not require any intricate equipment, and are easily automated [10].

It is known that the electrode material is the key parameter in optimizing the electrochemical process conditions: at around the oxygen evolution potential, the selectivity and efficiency of oxidation of organic compounds are determined by the ability of the anode material to adsorb $\cdot OH$ radicals [11].

On electrodes (active anodes), the concentration of $\cdot OH$ radicals chemisorbed on the surface is low, and organic compounds are oxidized selectively to give intermediate products [10]. On inactive anodes, $\cdot OH$ radicals are weakly bound to the electrode surface (physical adsorption), and, consequently, a full mineralization of organics can be achieved on anodes of this kind.

Lead dioxide (PbO_2) is a classical material with high oxygen evolution overvoltage and weak adsorption of $\cdot\text{OH}$ radicals. It is frequently used for oxidative destruction of various classes of organic compounds [7, 12–14].

Synthetic dyes belong to organic compounds with poor biodegradability, have one or two functional groups and complex aromatic structure, and can be used as model macromolecular pollutant compounds.

The goal of our study was to examine the kinetics and selectivity of the electrochemical oxidation of dyes [Methyl Orange (MO) and Chrome Dark Blue (CDB) on a lead dioxide anode (Pb/PbO_2) at various current densities, substrate concentrations, and pH values with the use of active oxygen species.

EXPERIMENTAL

Model solutions of Methyl Orange ($\text{C}_{14}\text{H}_{14}\text{N}_3\text{O}_3\text{SNa}$) and Chrome Dark Blue ($\text{C}_{16}\text{H}_9\text{ClN}_2\text{Na}_2\text{O}_4\text{S}_2$) were prepared by addition of a supporting electrolyte to an aliquot portion of a dye solution with known concentration. The initial concentrations of the dyes were 50 and 150 mg L^{-1} for MO and 150 and 200 mg L^{-1} for CDB. The corresponding values of the chemical oxygen demand (COD) were 65 and 190 mg O/L for MO and 115 and 150 mg O/L for CDB.

The experiments were performed in a single-chamber cell containing 150 mL of a solution under agitation with a magnetic stirrer at a temperature of 25–30°C. The following solutions served as the supporting electrolyte: 0.5 M Na_2SO_4 (pH 6) and a 3 : 1 mixture of 0.5 M Na_2SO_4 and 1 M H_2SO_4 (pH 2). The electrolysis was performed in the galvanostatic mode at current densities of 50, 100, and 125 mA cm^{-2} . A lead plate with working surface area of 4 cm^2 , on which a PbO_2 layer was deposited by the procedure described in [15], served as the working electrode (anode), and a graphite rod, as the cathode. The electrode potential of the anode was measured relative to a silver chloride reference electrode (s.c.e.). To stabilize the electrode surface and obtain reproducible results, Pb/PbO_2 was activated via polarization in 1 M H_2SO_4 alternately in the cathodic and anodic modes [16]. The following two schemes were used in oxidation of model dye solutions for generation of active oxygen species (AOS): anodic oxidation (AO) and anodic oxidation with portion-wise addition of H_2O_2 ($c_{\text{H}_2\text{O}_2} = 0.023 \text{ M}$) every hour (AO + H_2O_2).

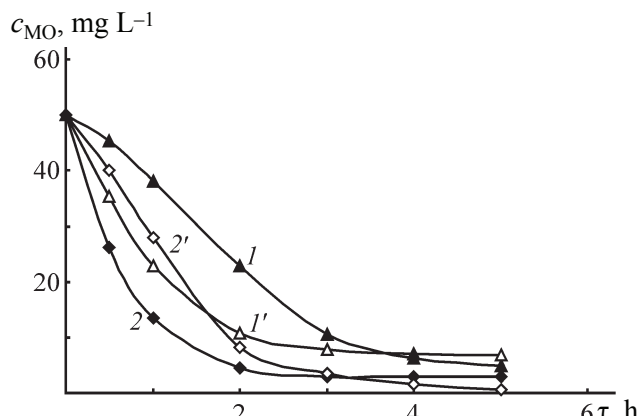


Fig. 1. Kinetic curves for MO oxidation on the Pb/PbO_2 electrode. (c_{MO}) MO concentration and (t) time. Current density 50 mA cm^{-2} , initial concentration 50 mg L^{-1} . (1, 2) AO, (1', 2') AO + H_2O_2 ; (1, 1') pH 6 and (2, 2') pH 2; the same for Fig. 2.

The dye concentrations in solution were determined by the photometric method [17], and the COD was measured by the reference method [18]. The composition of the oxidation products was analyzed by UV spectroscopy on a Cary 100 Scan spectrophotometer (Varian Inc.).

The kinetic curves of MO oxidation on the Pb/PbO_2 anode at a current density of 50 mA cm^{-2} and initial concentration of 50 mg L^{-1} ($\text{COD} = 65 \text{ mg O/L}$) are shown for various AOS generation schemes at pH 2 and 6 in Fig. 1. An analysis of the kinetic curves demonstrated that the initial anodic oxidation rate grows on passing from neutral to acid electrolyte, with addition of hydrogen peroxide raising the oxidation rate at pH 6 (curve 1') and exhibiting the opposite effect in an acid solution (curve 2'). It can be assumed that this deviation is due to the isomerization of the dye at various pH values due to the intramolecular rearrangement [19]. As a result, the composition and the reactivity toward both hydrogen peroxide and $\cdot\text{OH}$ radicals [20] of the intermediate products of its destruction may vary. In addition, it cannot be excluded that dyed intermediates raise the formation probability of colored intermediates raising the optical density of the solutions being analyzed, such as ortho-quinones [19]. It should be noted that the run of the dependences was preserved with increasing current density, whereas an increase in the initial MO concentration (decrease in the $\text{MO}/\text{H}_2\text{O}_2$ ratio) results in that the rate of the AO + H_2O_2 process becomes higher.

The results of MO oxidation for two AOS generation schemes at various current densities and dye concentrations are presented in Table 1.

An analysis of the values obtained for the MO oxidation efficiency demonstrated that a nearly full destruction

Table 1. Results of MO oxidation on the Pb/PbO₂ anode in 5 h of electrolysis

AOS generation scheme	Current density i , mA cm ⁻²	MO/COD concentration, mg L ⁻¹ /(mg O/L)			
		50/65		150/190	
		efficiency of MO oxidation, %	efficiency of COD reduction, %	efficiency of MO oxidation, %	efficiency of COD reduction, %
AO, pH 2	50	94.2	—	61.3	—
	100	96.0	69.2	73.3	51.0
	125	—	—	83.3	77.0
AO, pH 6	50	90.2	—	78.5	—
	100	97.5	75.0	90.6	66.7
	125	98.9	88.5	93.2	81.8
AO + H ₂ O ₂ , pH 2	50	86.2	—	69.1	—
	100	88.2	80.0	84.1	66.8
	125	—	—	91.6	82.5
AO + H ₂ O ₂ , pH 6	50	98.8	—	85.5	—
	100	100	87.5	94.7	83.3
	125	100	89.5	96.0	84.0

of the dye was observed in neutral solutions for both AOS generation schemes at $i = 100\text{--}125\text{ mA cm}^{-2}$. The efficiency of MO oxidation noticeably increased as the current density was raised from 50 to 100 mA cm⁻²: from 78.5 to 90.6% and from 85.5 to 94.7% for, respectively AO and AO + H₂O₂ at $c_0 = 150\text{ mg L}^{-1}$. Further increase in the current density to 125 mA cm⁻² changed the efficiency by only 2–3%.

As the initial dye concentration was raised to 150 mg L⁻¹, the influence exerted by the current density in the acid electrolyte was more pronounced for both the AO and AO + H₂O₂ schemes; nevertheless, the destruction efficiency did not exceed 92%.

The results obtained in determining the COD of the solutions upon oxidation indicate that, under the chosen conditions, it is impossible to reach the full MO mineralization: the efficiency of reducing the COD was 51 to 89.5%, depending on the process conditions. This is presumably due to the formation of intermediate, more oxidation resistant, dye destruction products, such as carboxylic acids [21], which is evidenced by UV spectroscopic data.

As the AOS concentration grows on raising the current density and(or) adding H₂O₂ to the solution bulk, the efficiency of COD reduction increases in both acid and neutral electrolytes, with this parameter being larger at pH 6.

The kinetic curves of CDB dye oxidation for various schemes of AOS generation and pH values at the initial dye concentration of 150 mg L⁻¹ and current density of 50 mA cm⁻² are shown in Fig. 2. It can be seen that the anodic oxidation rate of CDB is nearly independent of the electrolyte pH, whereas addition of H₂O₂ causes a decrease in the rate of its oxidation in the acid medium (curve 2'). It should be noted that the process kinetics was strongly affected by hydrogen peroxide during the initial period (1–2 h) of electrolysis at all the current densities and initial dye concentrations under study. For example, at the initial CDB content of 150 mg L⁻¹, its residual content after 1 h of electrolysis was 20 and 60 mg L⁻¹ at

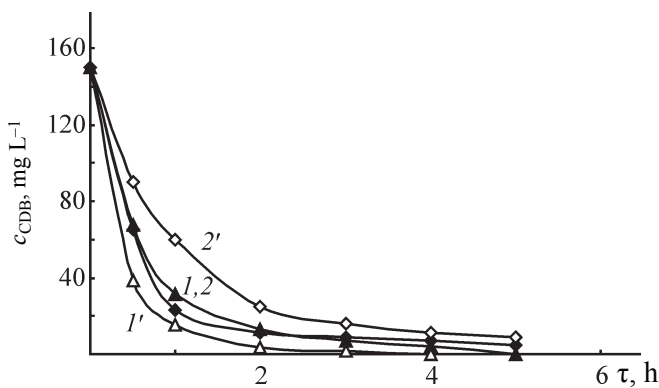


Fig. 2. Kinetic curves for CDB oxidation on the Pb/PbO₂ electrode. (c_{CDB}) CDB concentration and (τ) time. Current density 50 mA cm⁻², initial concentration 150 mg L⁻¹.

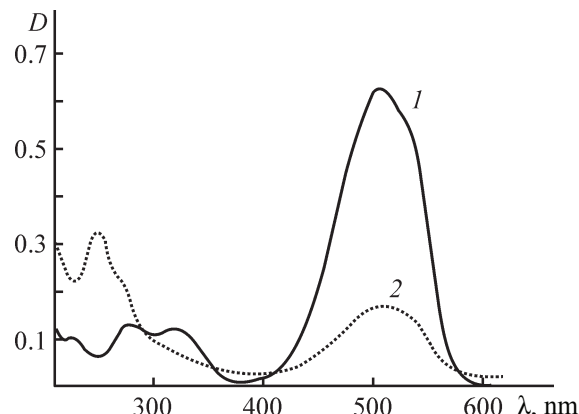


Fig. 3. Absorption spectra of MO oxidation products formed on a Pb/PbO₂ electrode. (D) Optical density and (λ) wavelength; the same for Fig. 4. (1) Starting compound and (2) that after 2 h of oxidation at a current density of 50 mA cm⁻² and initial concentration of 150 mg L⁻¹.

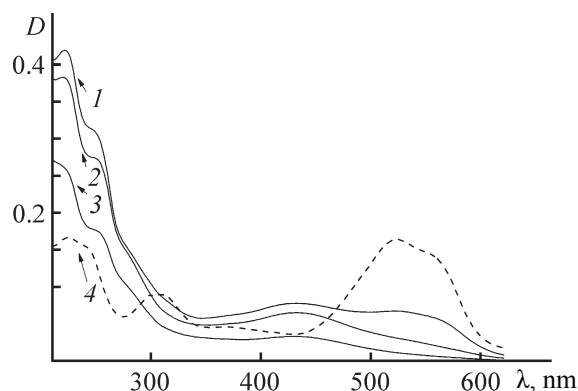
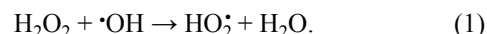


Fig. 4. Absorption spectra of CDB oxidation products formed on a Pb/PbO₂ electrode. Current density 125 mA cm⁻², initial concentration 150 mg L⁻¹. Electrolysis duration (h): (1) 0.4, (2) 0.75, (3) 2; (4) starting compound.

$i = 50 \text{ mA cm}^{-2}$ and 8 and 53 mg L⁻¹ at $i = 100 \text{ mA cm}^{-2}$ for AO and AO + H₂O₂, respectively. Raising the amount of AOS in the neutral solution made higher the destruction rate of the dye. The different effects of hydrogen peroxide on the oxidation kinetics at varied solution pH is possibly due to the various interaction rates of the intermediate products of CDB and H₂O₂ destruction, being formed in the solution bulk. In addition, hydrogen peroxide can enter in the case of the AO + H₂O₂ oxidation scheme into the reaction with ·OH radicals (scavenging effect) by

reaction (1) to give HO₂[•], which have a lower oxidizing capacity and higher selectivity than HO[•] [22]:



The calculated values of the efficiency of dye destruction and COD reduction are presented in Table 2.

It can be seen in Table 2 that the given type of dye is sufficiently effectively oxidized in 5 h of electrolysis under all the chosen conditions. It should be noted that

Table 2. Results of CDB oxidation on the Pb/PbO₂ anode in 5 h of electrolysis

AOS generation scheme	Current density i , mA cm ⁻²	CDB/COD concentration, mg L ⁻¹ /(mg O/L)			
		150/115		200/150	
		efficiency of MO oxidation, %	efficiency of COD reduction, %	efficiency of MO oxidation, %	efficiency of COD reduction, %
AO, pH 2	50	96.7	96.0	96.0	95.0
	100	100	99.0	99.0	99.0
	125	100	100	99.0	99.0
AO, pH 6	50	99.0 ($\tau = 4 \text{ h}$)	100	99.0 ($\tau = 4 \text{ h}$)	100
	100	100 ($\tau = 4 \text{ h}$)	100	99.0 ($\tau = 3 \text{ h}$)	100
	125	100 ($\tau = 4 \text{ h}$)	100	—	—
AO + H ₂ O ₂ , pH 2	50	94.0	94.0	97.0	95.0
	100	96.7	93.0	99.0	98.0
	125	100	100	—	—
AO + H ₂ O ₂ , pH 6	50	100 ($\tau = 4 \text{ h}$)	100	100 ($\tau = 4 \text{ h}$)	100
	100	—	—	—	—
	125	—	—	—	—

the time of the full CDB destruction in a neutral medium decreased to 3–4 h, depending on the current density.

The residual COD became smaller with increasing current density and decreasing initial CDB concentration, with the full mineralization of the dye observed in a neutral solution.

The UV spectroscopic data demonstrated that the dye destruction process occurs to give a number of intermediate products. Figures 3 and 4 show the absorption spectra of CDB and MO dyes, which have a characteristic strong absorption band peaked at 508 and 518 nm, respectively. The line shape of these absorption bands is due to the progression from vibrations of the N=N fragment contained in the dye molecules. In the course of electrochemical oxidation, this absorption band rather rapidly disappears, which is indicative of the effective destruction of this fragment. Along with that, additional absorption bands appear at shorter wavelengths, which is due to the appearance of low-molecular fragments and intermediate products formed in oxidation of the starting substrate. The following intermediate products are responsible for the following absorption bands (nm): 290–320 (quinoid structures, 270–280 (phenol-containing structures), and 250–260 (benzene derivatives). The last kind of organic products are carboxylic acids exhibiting a strong absorption at 200–210 nm.

CONCLUSIONS

(1) It was found that the electro-oxidation of Methyl Orange and Chrome Dark Blue on the Pb/PbO₂ anode occurs destructively via a number of intermediate products, which are further oxidized to CO₂, H₂O, and inorganic ions. The destruction efficiency of Methyl Orange in 5 h is 61 to 100%, and that of Chrome Dark Blue, 94–100%, depending on the current density, dye concentration, pH value, and generation scheme of active oxygen species.

(2) It was shown that Chrome Dark Blue is fully mineralized in 3–5 h, depending on the electrolysis conditions.

(3) It was found that the solution pH strongly affects the oxidation rate of the starting compounds during the initial period (1–2 h): the oxidation process of the chosen dyes occurs the most effectively in neutral solutions (pH 6).

REFERENCES

- Brillas, E., Baños, M.Á., Skoumal, M., et al., *Chemosphere*, 2007, vol. 68, pp. 199–209.
- Zarei, M., Niaezi, A., Salari, D., and Khataee, A.R., *J. Electroanal. Chem.*, 2010, vol. 639, pp. 167–174.
- Sánchez, A., Llanos, J., Sáez, C., et al., *Chem. Eng. J.*, 2013, vol. 233, pp. 8–13.
- Pacheco, M.J., Santos, V., Siríaco, L., and Lopes, A., *J. Hazard. Mater.*, 2011, vol. 186, pp. 1033–1041.
- Anotai, J., Lu, M.-C., and Chewpreecha, P., *Water Res.*, 2006, vol. 40, pp. 1841–1847.
- Vandevivere, P.C., Bianchi, R., and Verstraete, W., *J. Chem. Technol. Biotechnol.*, 1998, vol. 72, pp. 289–302.
- Morsi, M.S., Al-Sarawy, A.A., and Shehab El-Dein, W.A., *Des. Water Treat.*, 2011, vol. 26, pp. 301–308.
- Jain, R. and Shrivastava, M., *J. Hazard. Mater.*, 2008, vol. 152, pp. 216–220.
- Pirkarami, A., Olya, M.E., and Tabibian, S., *J. Environ. Sci. Health*, 2013, vol. 48, pp. 1243–1252.
- Martínez-Huitl, C.A. and Ferro, S., *Chem. Soc. Rev.*, 2006, vol. 35, pp. 1324–1340.
- Suna, J., Lua, H., Duc, L., et al., *Appl. Surf. Sci.*, 2011, vol. 257, pp. 6667–6671.
- Zhou, M., Dai, Q., Lei, L., et al., *Environ. Sci. Technol.*, 2005, vol. 39, pp. 363–370.
- Panizza, M. and Cerisola, G., *Ind. Eng. Chem. Res.*, 2008, vol. 47, pp. 6816–6820.
- Kornienko, V.L., Kolyagin, G.A., Kornienko, G.V., et al., *Russ. J. Appl. Chem.*, 2014, vol. 87, no. 1, pp. 1–5.
- Martínez-Huitl, C.A., De Battisti, A., Ferro, S., et al., *Environ. Sci. Technol.*, 2008, vol. 42, pp. 6929–6935.
- Kornienko, V.L., Chaenko, N.V., Kornienko, G.V., et al., *Russ. J. Appl. Chem.*, 2008, vol. 87, no. 8, pp. 1364–1368.
- Fisher, H., *Seminar po obshchei khimii: vvodnyi kurs po ekologicheski chistoj programme s eksperimental'nymi po regeneratsii khimicheskikh reagentov* (Workshop on General Chemistry: Introductory Course on an Environmentally Sound Program with Experimental on Regeneration of Chemical Reagents), Novosibirsk: Science, 2002.
- Fedorova, A.I. and Nikol'skaya, A.N., *Praktikum po ekologii i okhrane okruzhayushchey sredy* (Laboratory Course of Ecology and Environment Protection), Moscow: VLADOS, 2003.
- Kislenko, V.N. and Berlin, Ad.A., *Rus. Chem. Rev.*, 1991, vol. 60, no. 5, pp. 470–488.
- Enache, T.A. and Oliveira-Brett, A.M., *J. Electroanal. Chem.*, 2011, vol. 655, pp. 9–16.
- Brillas, E., Boye, B., Sirés, I., et al., *Electrochim. Acta*, 2004, vol. 49, pp. 4487–4496.
- Vysotskaya, N.A., *Rus. Chem. Rev.*, 1973, vol. 42, no. 10, pp. 851–856.